Analysis and Design of Sub-6 Beam Steerable Antenna Array Using Meta-material Loaded Vivaldi Elements.

A. khairy (Ahmed.khairy@eaeat.edu.eg)
Egyptian academy for engineering and advanced technology
A. Elboushi
Electronics Research Institute
A. A. Shaalan
Zagazig University
M. F. Ahmed
Zagazig University

Research Article

Keywords: Automotive antenna, Vivaldi antenna, Butler matrix, meta-material, Beam-steering.

Posted Date: June 23rd, 2022

DOI: https://doi.org/10.21203/rs.3.rs-1756851/v1

Additional Declarations: No competing interests reported.

Version of Record: A version of this preprint was published at Analog Integrated Circuits and Signal Processing on March 21st, 2023. See the published version at https://doi.org/10.1007/s10470-023-02156-w.

Abstract

in this paper, a sub-6 beam-steerable antenna array system is introduced. The main radiating element in the proposed array is a gain-enhanced Vivaldi antenna, whose overall realized gain is improved by introducing near-zero-index metamaterial [NZIM] with broadband characteristics at 3.6 GHz. The proposed system is intended to be integrated with fifth-generation (5G) automotive applications. The 4x4 butler matrix is resonating at 3.6 GHz to feed the designed antenna array elements and steer the radiating beam, which is suitable for automotive applications. All the system components, including antenna elements and the [4x4] butler matrix, are designed, simulated, and optimized by using CSTMWS 2020 and HFSS. In order to verify the proposed design, the system is fabricated using the photolithographic technique. The experimental results show very good agreement with the simulated ones. The NZIM-loaded antenna element achieves a -10 dB bandwidth of 2.9 GHz, while the overall array system achieves a 600 MHz bandwidth. The steered beam of the proposed system has an overall realized gain of 11.2 dB and covers an angle from 45^{o} to 135^{o}.

1. Introduction

Over recent years, automotive technology has been rapidly changing, which requires a significant increase in the data rate transferred. Development in the wireless network industry is becoming very necessary to meet the huge demand for such data rates. Many countries have adopted the fourth generation (4G) wireless communication system. However, some drawbacks, including overcrowded spectrum, high energy consumption, and high data rates, are not solved by 4G [1]. In comparison to the previous generation of 4G, 5G introduces significant differences and promises more benefits, such as wider bandwidth and less congested spectrum. The main goal of 5G technology is to improve the data rate by 1000 times compared to common communication standards and to connect 100 billion devices. The high data rates of several Gbps need even more support from the use of higher frequency bands, so 5G needs a wide spectrum across low, mid ,and high ranges to deliver widespread coverage and support all use cases. AutomotiveWireless communications include various applications, including automated driving of vehicles, driver assistance systems, vehicle-to-everything (V2X), vehicle-to-vehicle (V2V), and vehicle-to-infrastructure (V2I) [2]. The automotive applications need antennas that have some properties like beam steerable, wide bandwidth, and high realized gain. However, the automotive applications are loaded with optional antennas, so the proposed system is loaded with an antenna that has beam-steering, high gain, and wide bandwidth properties to work in different environmental conditions to cover important automotive services and support a high data transfer rate [3]. Antenna-array systems with butler-matrix are one of the methods to achieve the desired aims. In this paper, the single-element antenna is a Vivaldi, which was suggested by Gibson [4]. The single element is loaded with NZIM to improve the overall realized gain [5]. Beam steering is a technique to steer the beam by controlling the phase of each element. The [4x4] butler matrix is optimized for this aim [6, 7].

2. Single Element Design

A single Vivaldi element is designed and optimized to operate at 3.6 GHz with broadband characteristics. The Vivaldi antenna meets the desired purpose [8]. Roger RT5880 with relative permittivity ($\varepsilon_r = 2.2$), a thickness of .787mm, and low tangent losses ($\tan \delta = .0009$) is chosen for sub-6 antennas to reduce losses, especially in antennas that operate at high frequencies. The single element geometry is shown in Fig. 1. The proposed design dimensions are presented in Table 1. Also, the simulated return loss S_{11} is shown in Fig. 2. CSTMWS 2020 and HFSS, two software packages that differ in their simulation techniques, were used to simulate the proposed designed system [9].

Table 1
The Optimized Dimensions of Proposed Vivaldi Antenna.

parameter	*ws*	*Lt*	*Lp*	*Ln*	*Lc*	*S*	*Wq*	*D*	*Rs*	*Rw*	*Sd*	*r*	*a*
Value (mm)	*86*	*80.30*	*68.80*	*8.60*	*39.11*	*12.58*	*1.20*	*4.80*	*2.45*	*2.64*	*1.20*	*15*	*90°*

The results simulated by the two programs are close to the measured results, achieving a -10 dB bandwidth of 2.9 GHz for a single Vivaldi element.

3. Near-zero-index Metamaterial [nzim]

The phase velocity of propagating electromagnetic waves tends to infinity in the NZIM metamaterials. As a result, the final wavelength also tends to infinity. The NZIM metamaterial is used as a high refractive index impact to result in a confined pattern and high directivity [10]. Also, by providing a high-refractive-index effect, the metamaterial is intended to replace dielectric lenses for gain enhancement [10]. So, the NZIM units use the same thickness of dielectric material to be introduced within the front of a Vivaldi antenna [11, 12]. The NZIM metamaterial is used in essential applications such as producing unwanted impedance mismatch in the desired system [13]. The unit cell dimension is optimized and simulated using CSTMWS 2020. The NZIM unit cell dimensions are *(*Ls *= 7mm*, Lm *= 6mm, and* Wx *= 0.5mm)* as shown in Fig. 3.

The value of the n index is approximately near zero, its real value is 0.1885, and the image value is zero. The designed element of the Vivaldi antenna aperture is filled with NZIM to improve the overall realized gain, as shown in Fig. 4.

It was required to analyze the impact of the NZIM units on the realized gain after they were added to the proposed single element. Hence, the realized gain versus frequency is simulated using CSTMWS 2020 in Fig. 5.

The value of the maximum overall realized gain is 8.6418 dB at a frequency of 3.6 GHz when three columns of the NZIM unit cells are added to a single Vivaldi element. The NZIM unit cells achieve a confined pattern with high directivity and increase the overall realized gain by 1.12 dB.

4. Butler Matrix Components Design.

Beam-steering is one of the important properties in automotive communications. The proposed system is fed by a Butler matrix, which is considered a passive beam-steering network. The Butler matrix was proposed by Butler and Lowe in 1961. It consists of a 90° hybrid Coupler, crossover, and phase shifter[14].

4.1. 90° Hybrid Coupler

A hybrid coupler is a passive four-port network, as shown in Fig. 6, that splits the input power into two equal-power signals at the outputs, and the fourth port is isolated. The coupling is 3 dB and half-power split at the outputs. For a 90° hybrid coupler, the outputs differ in phase by 90° [6, 14].

The 3-dB coupler is designed in HFSS and CSTMWS 2020 to obtain the S-parameters, and phase difference between coupled ports as shown in Fig. 7.

4.2. Crossover

The crossover is optimized with a high level of isolation between the input ports to avoid overlapping signals during crossings. It is simple to construct by cascading two-hybrid 3-dB couplers [15]. The designed crossover and simulated results with good isolation between ports are shown in Fig. 8.

4.3. Phase shifter

In the designed system, phase shifters are critical components. The power at the output of the micro-stripline phase shifter should be identical to the input power, implying a 0 dB insertion loss. However, there are dielectric and conductor losses that degrade the insertion loss owing to the non-ideal transmission line length [16]. At higher frequencies, these losses are more pronounced. The phase difference between the input and output ports can be easily changed by changing the electrical length of the line [7].

4.4. The [4x4] Butler matrix

The butler matrix is designed, optimized, and fabricated. The simulation results are obtained using CSTMWS 2020 and HFSS. The output ports are separated by ($\lambda o/2$), which is equal to approximately 42 mm at an operating frequency of 3.6 GHz to avoid mutual coupling between array elements. The proposed design layout is shown in Fig. 9.

The results for the [4x4] butler matrix phase difference between output ports simulated by using CSTMWS 2020 and HFSS are shown in Fig. 10.

5. System Design And Result For Discussion.

In this section, the complete designed system results are obtained by using the Advanced Design System (ADS 2019) simulator to show mutual coupling between input ports and return loss for input ports [17]. The results were presented in Fig. 12 and compared with the measured ones. The data is extracted from CSTMWS 2020 (Touchstone files) and is used to obtain results in ADS 2019 as shown in Fig. 11.

The results obtained by ADS 2019 are approximately as measured. To achieve beam steering, the phase of the input signal is adjusted for all radiating components [18, 19].As shown in Table 2, the Butler matrix achieves this goal. Also, Fig. 13 shows beam steering simulated results by using CSTMWS 2020 compared to measured results.

Table 2
The phase difference between ports by using CSTMWS 2020 at an operating frequency of 3.6 GHz.

cases:	*case 1*	*case 2*	*case 3*	*case 4*
port Excitation	*port (p1)*	*port (p2)*	*port (p3)*	*port (p4)*
port (p5)	*-108.239*	*-6.401*	*-60.390*	*30.313*
port (p6)	*-66.042*	*-154.906*	*65.874*	*-20.218*
port (p7)	*-20.218*	*65.874*	*-154.906*	*-66.042*
port (p8)	*30.313*	*-60.390*	*-6.400*	*-108.239*

At the operating frequency of 3.6 GHz, the maximum measured realized gain is 11.2 dB, and the butler matrix enabled the system to cover an angle from 45^o to 135^o, which steered the beam in the desired direction as shown in

Fig. 13. Also, the proposed system achieves a -10 dB bandwidth of 600 MHz as shown in Fig. 12. The high gain, wide bandwidth, and beam steering technology in the designed system make communications possible in remote locations and critical environmental conditions for automotive applications. Beam steering in automotive applications helps to reduce multipath fading occurrences by forming the beam in the desired direction to avoid interference and noise sources. In addition, steerable antennas enable sensors to achieve longer ranges, higher data rates, and lower power consumption (longer battery life) [20, 21].

6. Conclusion

In this paper, the proposed design is simulated and fabricated, showing good results. The proposed single Vivaldi element supports the entire sub-6 GHz frequency bands and is loaded by the NZIM units to increase overall realized gain. The passive beam steering network is a butler matrix, which is optimized at an operating frequency of 3.6 GHz with good isolation between ports and covers an angle from 45^{o} to 135^{o}. The proposed system has some properties that support automotive applications, such as high gain, wide broadband, and the property of beam steering. Automotive applications are becoming increasingly important in our life, and include very essential services such as v2x, v2v, and global positioning system (GPS), so the proposed system can be considered as a good candidate for this purpose.

Declarations

Acknowledgments: The authors would like to thank Prof. Dr. Fawzy Ibrahim, Dean of the Egyptian Academy for Engineering and Advanced Technology, as well as the Ministry of State for Military Production for making available the measurements of fabricated circuits.

Author Contribution: All authors contributed to the study's conception and design. Abdel-Hamid Shaalan developed the final vision for the study as well as reviewed the work. Circuit preparation, data collection, and analysis performed by Ahmed Khairy. The first draft of the manuscript was written by Ahmed Khairy, Ayman Elboushi, and Mai Ahmed. All authors commented on previous versions of the manuscript.

Funding: No funding from an individual or organization.

Declarations: Availability of data and material upon request.

Conflict of Interest: The authors declare that they have no conflict of interest.

References

1. P. Gupta, L. Malviya, S. J. I. J. o. M. Charhate, and W. Technologies, "5G multi-element/port antenna design for wireless applications: a review," vol. 11, no. 9, pp. 918-938, 2019.
2. C. R. Storck and F. J. I. A. Duarte-Figueiredo, "A survey of 5G technology evolution, standards, and infrastructure associated with vehicle-to-everything communications by internet of vehicles," vol. 8, pp. 117593-117614, 2020.
3. V. Rabinovich and N. Alexandrov, *Antenna arrays and automotive applications*. Springer Science & Business Media, 2012.
4. P. J. Gibson, "The vivaldi aerial," in *1979 9th European Microwave Conference*, 1979, pp. 101-105: IEEE.

5. D. Sarkar and K. V. Srivastava, "Four element dual-band sub-6 Ghz 5G MIMO antenna using SRR-loaded slot-loops," in *2018 5th IEEE Uttar Pradesh Section International Conference on Electrical, Electronics and Computer Engineering (UPCON)*, 2018, pp. 1-5: IEEE.
6. V. Prakash, S. Dahiya, S. Kumawat, and P. J. P. I. E. R. C. Singh, "Design of 4× 4 Butler Matrix and its Process Modeling Using Petri Nets for Phase Array Systems," vol. 103, pp. 137-153, 2020.
7. I. Uchendu and J. R. J. P. I. E. R. B. Kelly, "Survey of beam steering techniques available for millimeter wave applications," vol. 68, pp. 35-54, 2016.
8. M. M. Honari, M. S. Ghaffarian, and R. J. E. Mirzavand, "Miniaturized antipodal vivaldi antenna with improved bandwidth using exponential strip arms," vol. 10, no. 1, p. 83, 2021.
9. Z. Cendes, "The development of HFSS," in *2016 USNC-URSI Radio Science Meeting*, 2016, pp. 39-40: IEEE.
10. A. Alu, M. G. Silveirinha, A. Salandrino, and N. J. P. r. B. Engheta, "Epsilon-near-zero metamaterials and electromagnetic sources: Tailoring the radiation phase pattern," vol. 75, no. 15, p. 155410, 2007.
11. B. Zhou, H. Li, X. Zou, and T.-J. J. P. I. E. R. Cui, "Broadband and high-gain planar Vivaldi antennas based on inhomogeneous anisotropic zero-index metamaterials," vol. 120, pp. 235-247, 2011.
12. T. Zhang, J. Zhao, Y. Guo, X. J. I. M. Zhao, Antennas, and Propagation, "High-gain omnidirectional patch antenna for conformal application based on near-zero-index metamaterials," vol. 15, no. 12, pp. 1649-1656, 2021.
13. S. El-Nady, H. M. Zamel, M. Hendy, A. A. Zekry, and A. J. P. I. E. R. C. Attiya, "Gain enhancement of a millimeter wave antipodal vivaldi antenna by epsilon-near-zero metamaterial," vol. 85, pp. 105-116, 2018.
14. A. K. Vallappil, M. K. A. Rahim, B. A. Khawaja, N. A. Murad, and M. M. J. I. A. Gajibo, "Butler Matrix Based Beamforming Networks For Phased Array Antenna Systems: A Comprehensive Review and Future Directions For 5G Applications," 2020.
15. M. Moubadir, H. Aziz, N. A. Touhami, M. Aghoutane, K. Zeljami, and A. Tazón Puente, "Design and implementation of a technology planar 4x4 butler matrix for networks application," 2015.
16. E. J. J. I. T. o. M. T. Denlinger and Techniques, "Losses of microstrip lines," vol. 28, no. 6, pp. 513-522, 1980.
17. F. Benzerga, M. Abri, and H. Badaoui, "Analysis and Design of Vivaldi Antipodal (Antenna array AVA) for Passive Imaging Applications."
18. M. H. Habaebi, M. Janat, and M. R. J. P. I. E. R. M. Islam, "Beam steering antenna array for 5G telecommunication systems applications," vol. 67, pp. 197-207, 2018.
19. I. Ahmed *et al.*, "A survey on hybrid beamforming techniques in 5G: Architecture and system model perspectives," vol. 20, no. 4, pp. 3060-3097, 2018.
20. A. Pal, A. Mehta, D. Mirshekar-Syahkal, H. J. I. T. o. A. Nakano, and propagation, "A twelve-beam steering low-profile patch antenna with shorting vias for vehicular applications," vol. 65, no. 8, pp. 3905-3912, 2017.
21. H. Wymeersch, G. Seco-Granados, G. Destino, D. Dardari, and F. J. I. W. C. Tufvesson, "5G mmWave positioning for vehicular networks," vol. 24, no. 6, pp. 80-86, 2017.

Figures

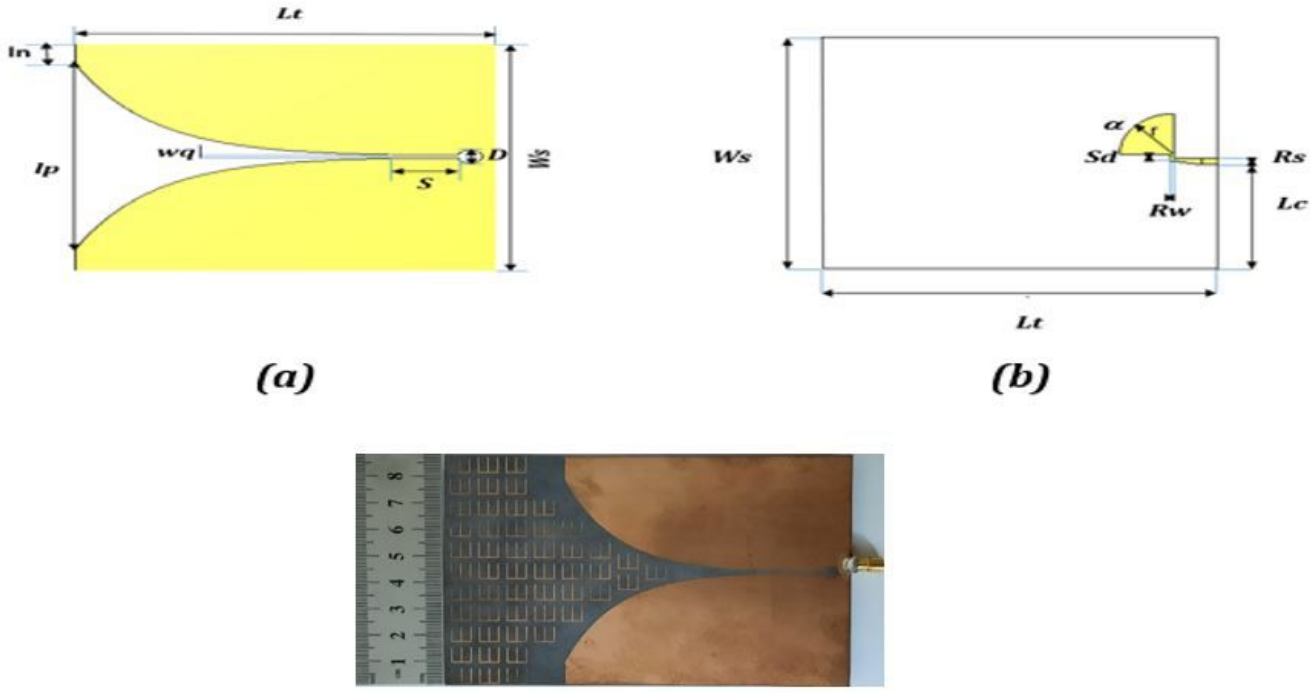

Figure 1

The Geometry of the Proposed Vivaldi Antenna: (a) Top view and (b) Bottom view

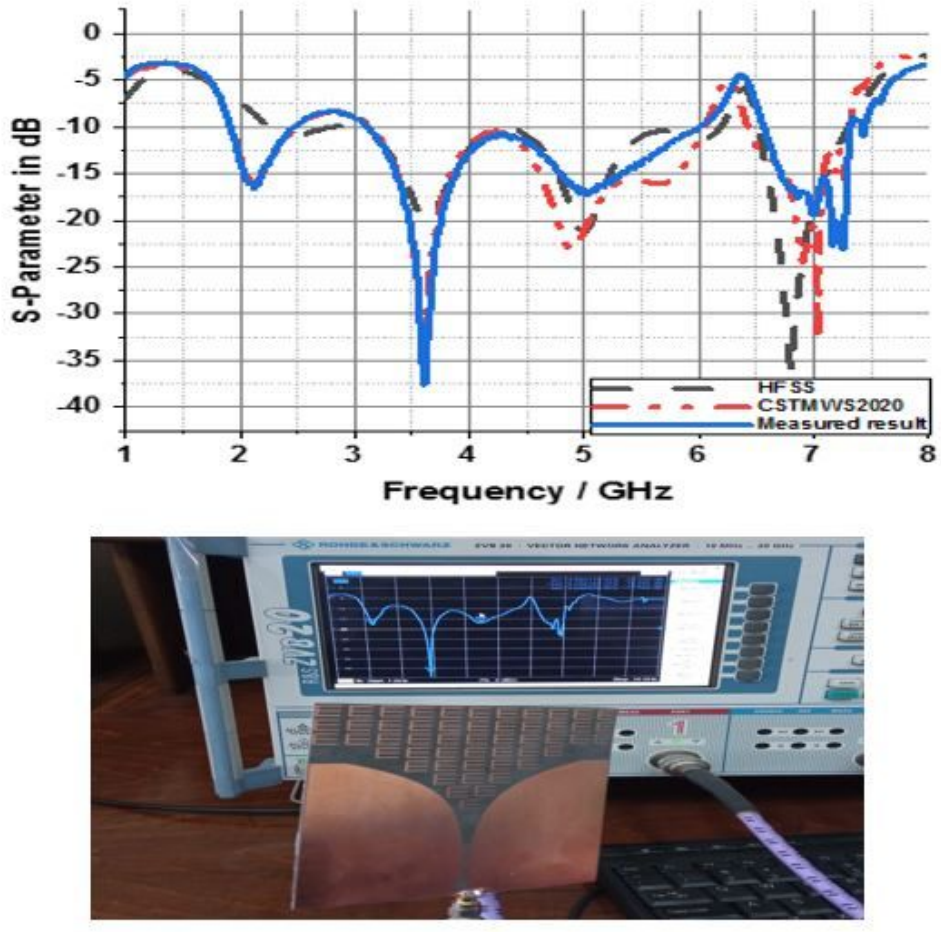

Figure 2

The Simulated and measured return loss S_{11} for the Proposed Vivaldi Antenna.

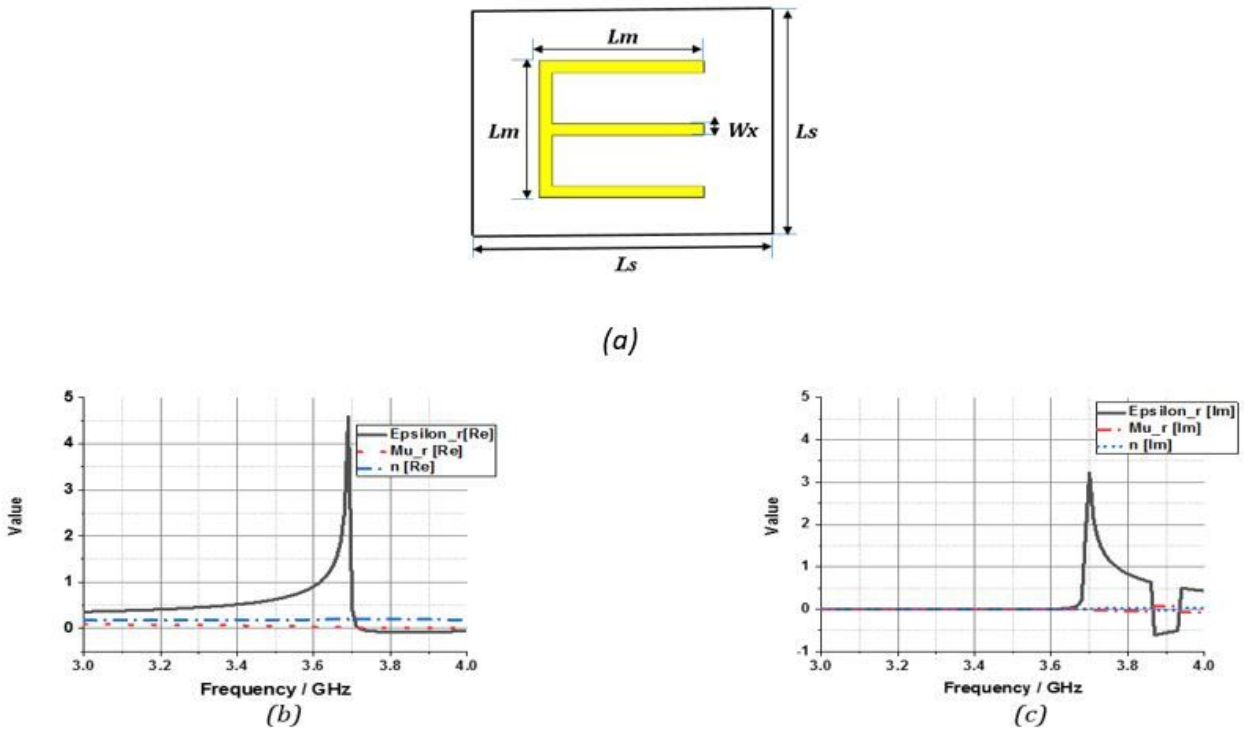

Figure 3

a) The Geometry of Proposed NZIM unit cell. (b) The real part of ε_r, μ_r, and refractive index n. (c) Image part of ε_r, μ_r, and refractive index (n).

Figure 4

(a) The Proposed designed antenna with embedded NZIM meta-material, (b) Electric Field distribution when using (2) columns of NZIM.

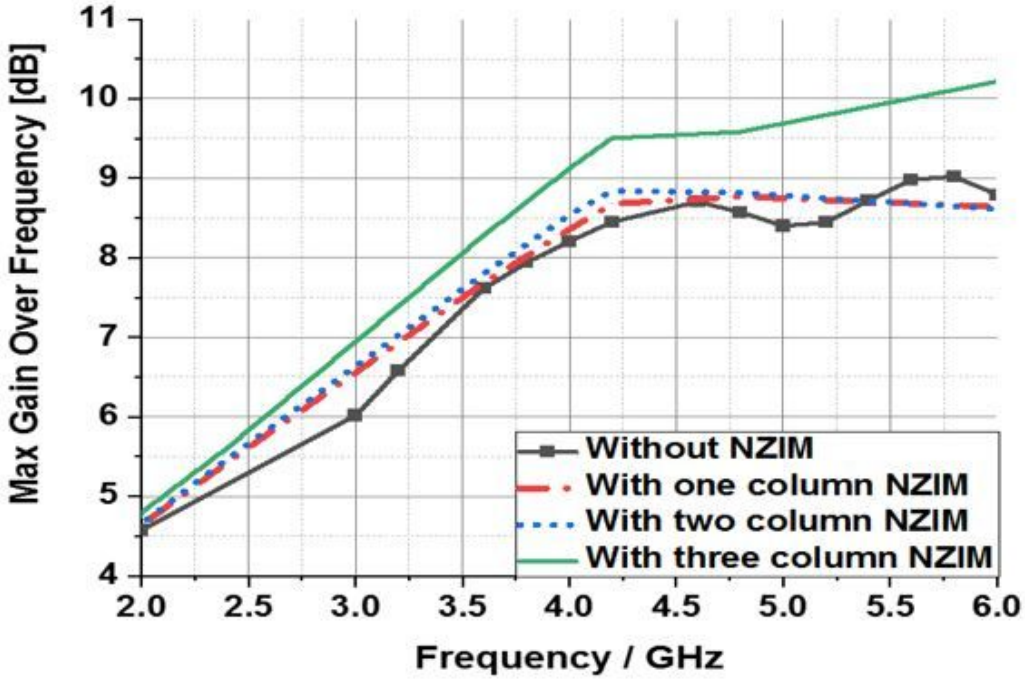

Figure 5

The maximum realized gain versus frequency of a single Vivaldi element for various numbers of columns introduced within the front of the Vivaldi antenna element.

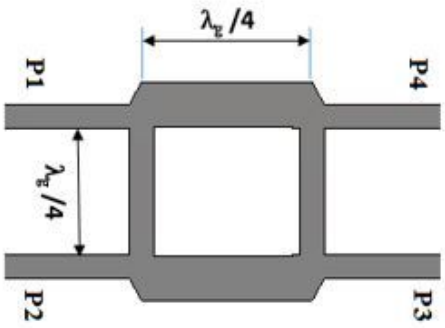

Figure 6

The layout of the 3 dB coupler.

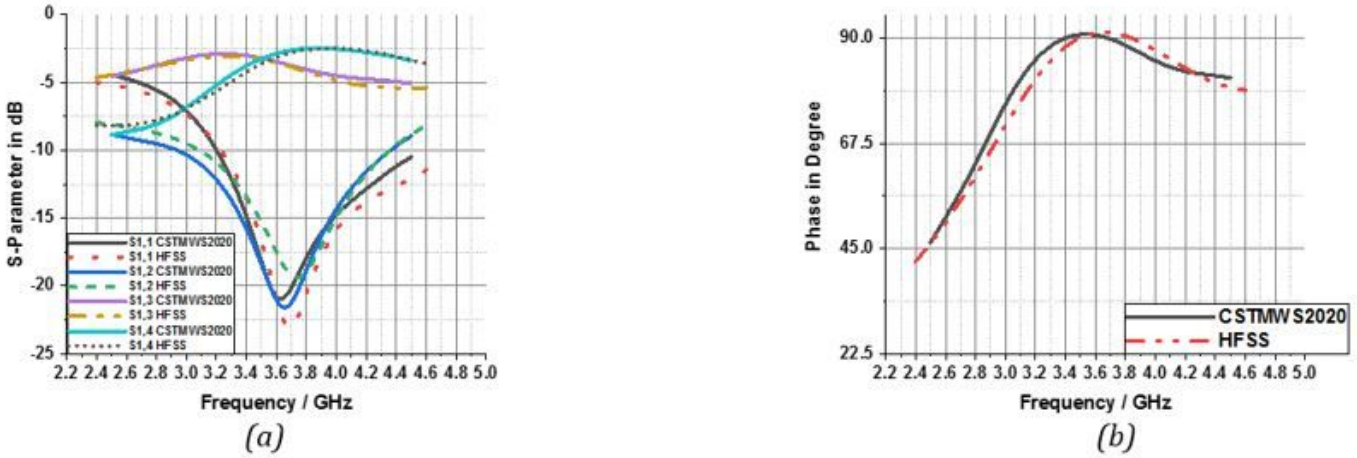

Figure 7

(a) The reflection coefficient of 3 dB coupler. (b) The phase difference between output ports, which is 90.4^{o} at an operating frequency of 3.6 GHz.

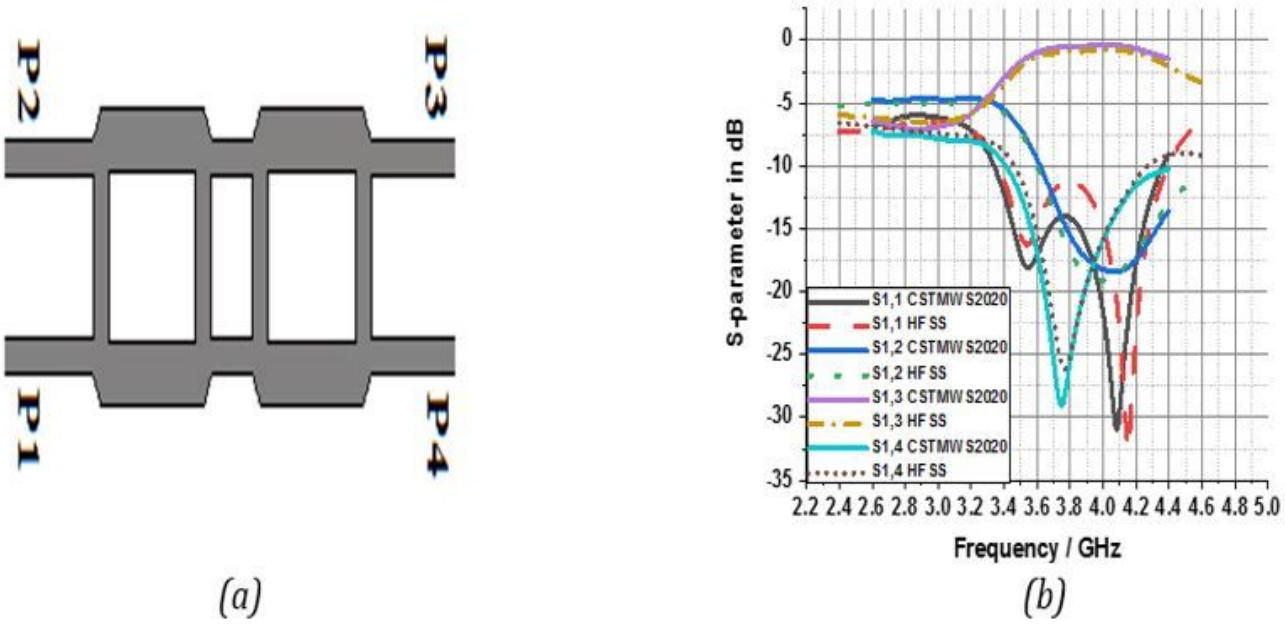

Figure 8

(a) The Layout of the crossover and (b) the results of the reflection coefficient.

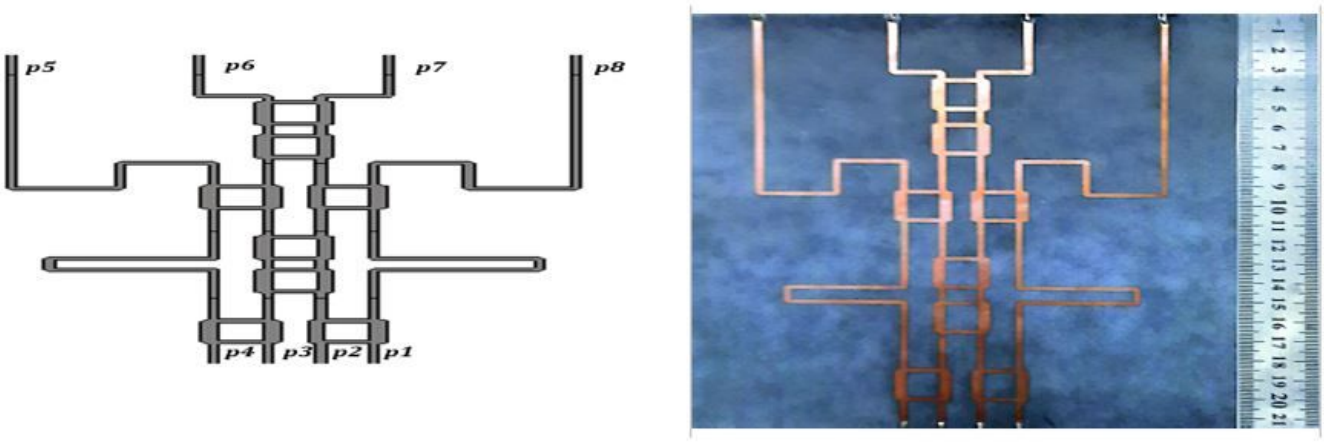

Figure 9

The designed layout of the butler matrix.

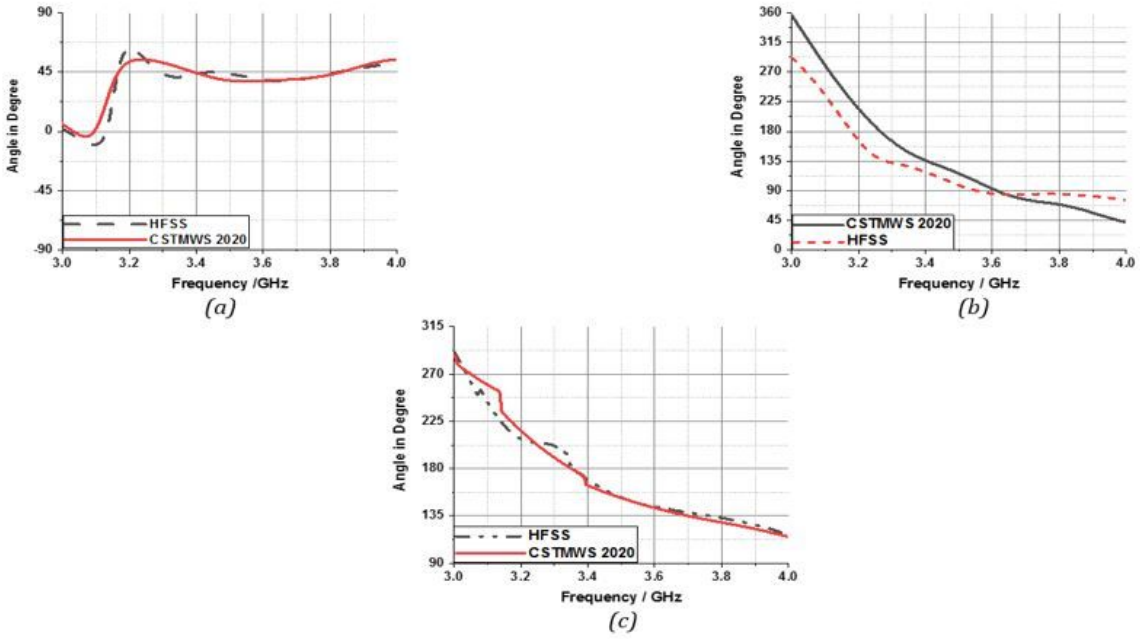

Figure 10

The phase difference between output ports with respect to port 8 (p8). (a) In this case phase differences equal 45^{o}, (b) 90^{o}, and (c) 135^{o}.

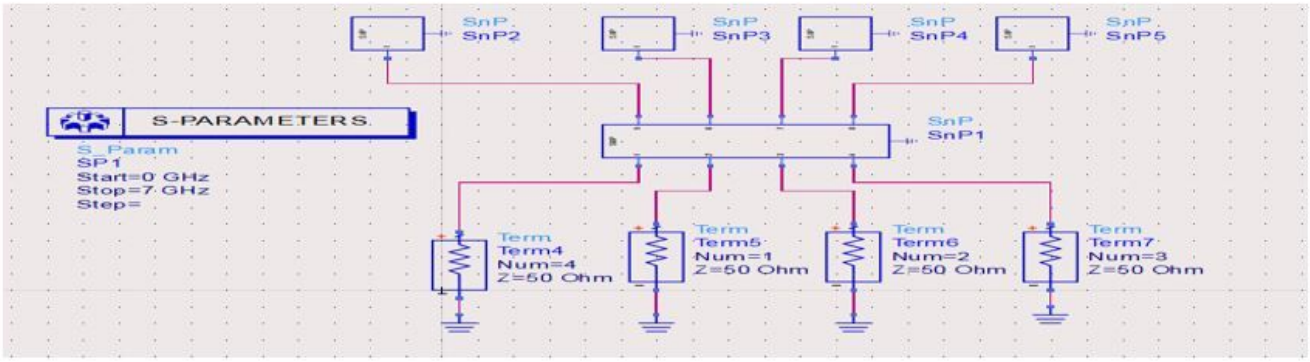

Figure 11

The complete designed system data diagram in the ADS 2019 simulator.

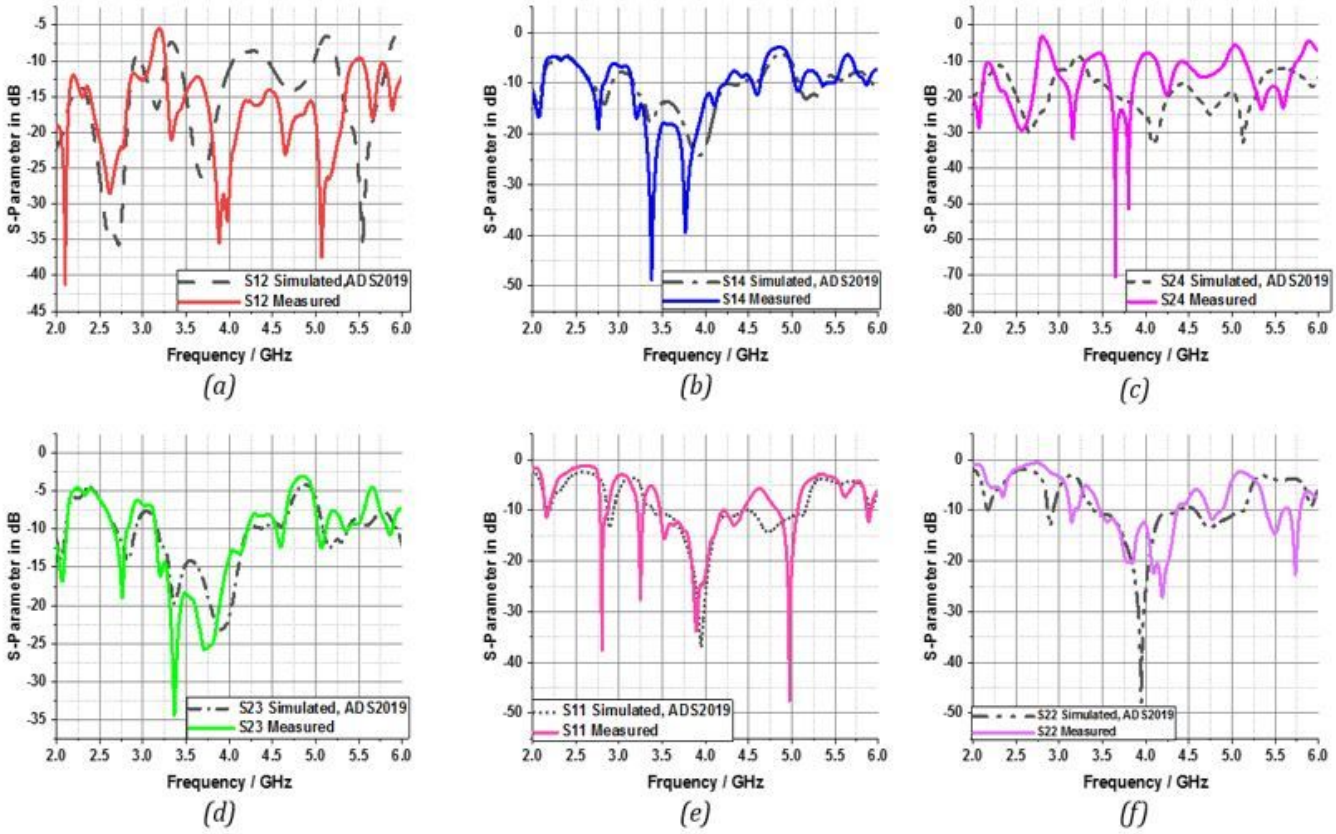

Figure 12

(a), (b), (c), and(d) are the mutual coupling between input ports of the designed system, which is less than -10 dB. (e), and (f) is the return loss of the designed system.

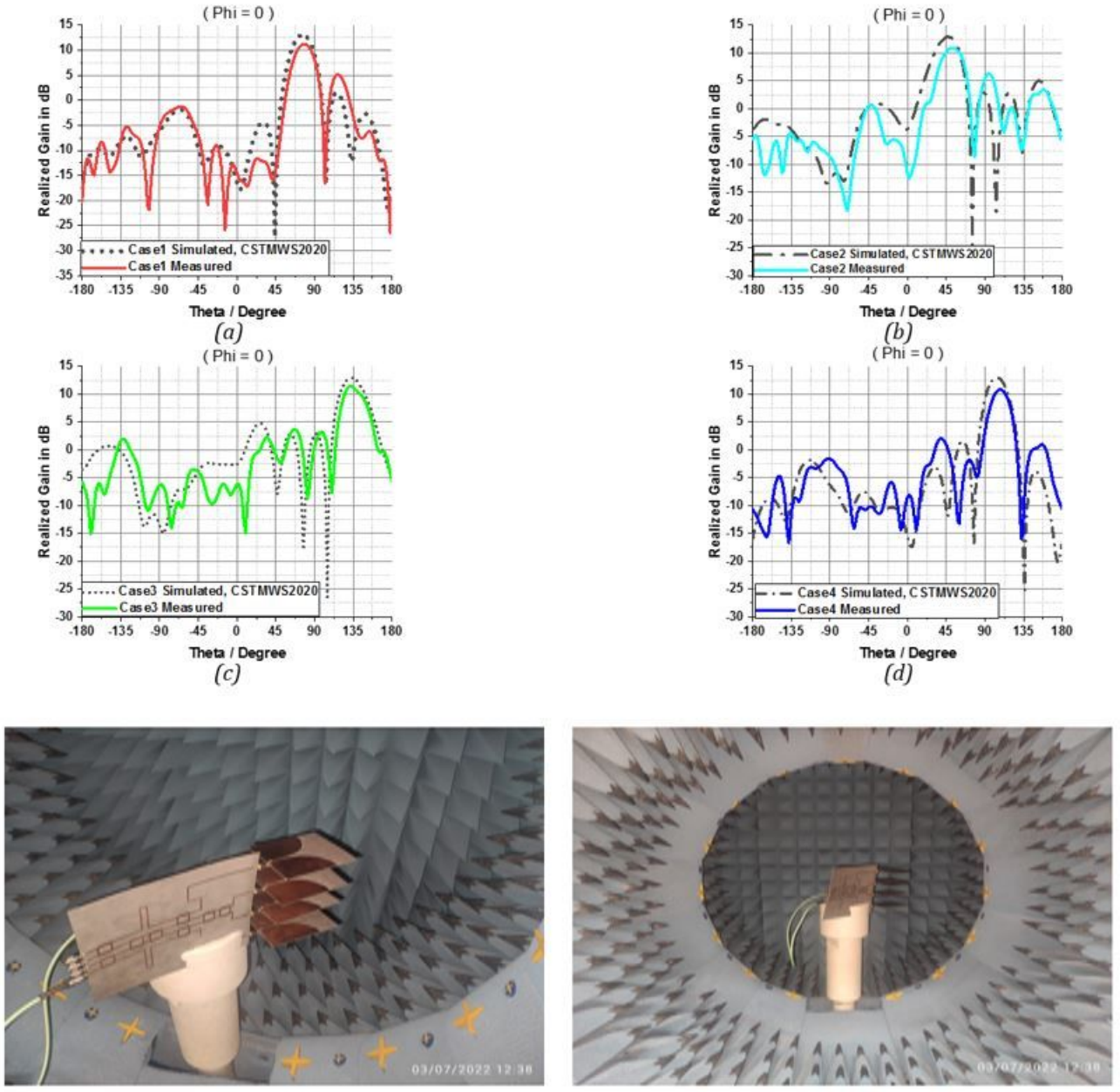

Figure 13

The realized gain versus theta in different cases by changing the input port, which leads to beam steering in cases (a), (b), (c), and (d).